Electrical Conductivity through a Single Atomic Step Measured with the Proximity-Induced Superconducting Pair Correlation

Howon Kim, Shi-Zeng Lin, Matthias J. Graf, Yoshinori Miyata, Yuki Nagai, Takeo Kato, and Yukio Hasegawa

Phys. Rev. Lett. **117**, 116802 — Published 8 September 2016

DOI: 10.1103/PhysRevLett.117.116802

Electrical conductivity through a single atomic step measured with the proximity-induced superconducting pair correlation

Howon Kim[1†], Shi-Zeng Lin[2], Matthias J. Graf[2§], Yoshinori Miyata[1], Yuki Nagai[3], Takeo Kato[1], and Yukio Hasegawa[1*]

[1]The Institute for Solid State Physics, The University of Tokyo, 5-1-5, Kashiwa-no-ha, Kashiwa, 277-8581 Japan
[2]Theoretical Division, Los Alamos National Laboratory, Los Alamos, New Mexico 87545, USA
[3]CCSE, Japan Atomic Energy Agency, Kashiwa, Chiba 277-8587, Japan

* e-mail address: hasegawa@issp.u-tokyo.ac.jp
† present address: Department of Physics, University of Hamburg, D-20355 Hamburg, Germany
§ present address: Office of Science, U.S. Department of Energy, Washington, DC 20585-1290, USA

Abstract: Local disordered nanostructures in an atomically thick metallic layer on a semiconducting substrate play significant and decisive roles in transport properties of two-dimensional (2D) conductive systems. We measured the electrical conductivity through a step of monoatomic height in a truly microscopic manner by using as signal the superconducting pair correlation induced by the proximity effect. The transport property across a step of a one-monolayer Pb surface metallic phase, formed on a Si(111) substrate, was evaluated by inducing the pair correlation around the local defect and measuring its response, *i.e.* the reduced density of states at the Fermi energy using scanning tunneling microscopy. We found that the step resistance has a significant contribution to the total resistance on a nominally flat surface. Our study also revealed that steps in the 2D metallic layer terminate the propagation of the pair correlation. They enhance superconductivity between the first surface step and the superconductor / normal metal interface by reflectionless tunneling when the step is located within a coherence length.

PACS: 73.25.+i, 74.45.+c, 68.37.Ef

The recent discovery of monolayer (ML) superconductivity [1-3] revived the research on one-atom-thick metal layers formed on semiconductor surfaces. Electronically decoupled from the substrate, the metallic overlayers hold an ultimately-thin two-dimensional (2D) electron system, and combined with the broken inversion symmetry, they exhibit various fascinating features, such as giant Rashba spin-split states [4,5] including one showing superconductivity [6], and valley spin polarized states [7]. For these 2D systems, atomic steps on the substrate, whose presence is ubiquitous and unavoidable, play a significant role in the transport properties [3]. For the characterization of electrical conductivity, an electrical current is injected from one side of the object and the transmitted one is detected in the other side. It is, however, technically very difficult to measure transport on such nano-scale structures. In this Letter, we report on measurements of the electrical conductivity through a single ML-high step on a 2D metallic layer by inducing the superconducting pair correlation through the proximity effect, and by detecting its signal in tunneling spectra measured by scanning tunneling microscopy and spectroscopy (STM/STS).

The propagation of the pair correlation from a superconductor / normal metal (SN) interface into the normal metal has been investigated by using STM/STS [8-14]. Near the interface in the normal metal, the single particle spectrum shows a dip at the Fermi energy (E_F), which is a good measure of the superconducting pair correlation. [15, 16] Through spatial mapping of the density of states (DOS) at E_F with nanometer spatial resolution, one can learn how the pair correlation is distributed in the normal metal. In general, the pair correlation decays with distance from the SN interface. By placing a surface step within the decay length the pair correlation can be induced there, and we use STM/STS to investigate how superconductivity is affected by the presence of steps. In fact, the proximity-induced pair correlation has been utilized to create novel electronic states, such as *p*-wave and odd-frequency superconductivities [17, 18]. It is also one of the key ingredients for the stabilization of the Majorana bound states [19-22], which are promising building blocks for quantum computing. Thus elucidating the role of local disordered nanostructures on the distribution of the pair correlation has significant implications on the creation, modification, and control of these elusive states.

We probed the pair correlation around an interface between a superconducting

crystalline Pb island and a striped incommensurate (SIC) phase by taking tunneling spectra using low-temperature STM. The SIC phase, a ML Pb-induced surface-reconstructed structure formed on Si(111) surface, is a 2D normal metal at our measurement temperature (2.15 K). The phase exhibits superconductivity below the critical temperature (See S1 in Supplemental Materials (SM) [23] for measured superconducting gap), which is reported as 1.83 K and 1.1 K according to STM [1] and electrical conductance [2] measurements, respectively. The surface metallic phase was prepared *in situ* by 1.5 ML-Pb deposition at room temperature onto a Si(111) substrate (As doped, 1-3 mΩ·cm) followed by annealing at 640~660 K [24]. In order to form Pb islands, Pb was again deposited on the SIC phase at 240 K. Mechanically polished PtIr tips were used as probes. All the differential tunneling conductances were measured in a standard lock-in method whose modulated sample bias voltage is 100 μV_{RMS} at 2 kHz, while the tunneling junction was stabilized with the sample bias voltage V_S of 5 mV and tunneling current I_T of 400 pA.

Figure 1(a) is an STM image showing an 8 ML Pb island on an SIC phase. Tunneling spectra taken along the line drawn in the STM image, shown in the inset, indicate a superconducting gap in the Pb island and no gap in the SIC phase far from the island. In the SIC phase near the island a suppressed gap, induced by the proximity effect, can be seen, and the depth in the DOS at E_F decays with distance from the interface. However, no minigap is observed. A tiny V-shaped pseudogap feature in the normal-metal layer far from the island was observed even without Pb islands. This pseudogap has been studied in other atomically thin conventional superconductors [25] and is thought to be due to the dynamical Coulomb blockade (DCB) [9, 26]. For a quantitative analysis of the gap's decay profile in the DOS, we plotted the value of negative zero-bias conductance (ZBC) in Fig. 1(b). It was normalized by the ZBC value measured on the normal metal 200 nm away from the SN interface to make it 0 (-1) in the superconducting (normal metal) area and to eliminate the DCB effect. From an exponential fit, drawn with a red line in the plot, we found the decay length $\xi = 40.5 \pm 1.7$ nm, consistent with previous results [8, 11].

Figure 1(c) shows tunneling spectra taken in the proximity area. In order to quantitatively explain the spectra, we performed a numerical analysis using the Usadel

equation [27-29] (See Sec. 3 in the SM for details [23]), which has been utilized for the analysis of the proximity effect on diffusive metals including the present system [8, 11]. The estimated mean free path is 4.3 nm (See Sec. 2 in the SM for detailed calculations [23]), which is much shorter than the coherence length ξ and indicates that the system is in the dirty limit. We calculated tunneling spectra using Eq. S3 and multiplied them by a spectrum taken at 178 nm from the SN interface to incorporate the DCB effect. The calculated spectra are white lines superimposed on the experimental curves, demonstrating good agreement. From the calculations, the ratio of the electrical conductivity through the SN interface to the normal metal conductivity σ_{SN}/σ_N was estimated as 38 μm^{-1}.

To measure the step conductivity we investigated the spatial distribution of the pair correlation around steps of the normal-metal layer close to superconducting islands. Figure 2(a) is an STM image showing 9-22 ML high Pb islands, elongated along the step-edge direction, formed on a stepped SIC phase. The ML-high steps, marked with black-dashed lines, are aligned from the left side of the image down to the right. Since the growth of the islands tends to be initiated / terminated at the steps, the islands' edges, marked with white-dashed lines, often overlap with them. At every pixel of the area we measured the ZBC, its spatial map is presented in Fig. 2(b). In the conductance map all Pb islands are colored green, which indicates zero ZBC and fully gapped superconductivity there. The 2D metallic layer far from the Pb islands is colored yellow, indicating a normal metal with no gap. The area surrounding the Pb islands is colored blue to red, implying a reduced DOS at E_F due to the proximity effect.

We found from the ZBC maps that the steps terminate the propagation of the pair correlation into adjacent terraces. Both the upward and downward steps work as terminators. The cross-sectional plot of the ZBC (upper panel) and topography (lower panel) along the line aa', shown in Fig. 2(c), exhibits the decay of the ZBC in the SIC terrace in vicinity of the Pb island and its sudden disappearance beyond the step edge. Previous studies reported that steps themselves do not cause pair breaking [10]. Since surface steps break the translational symmetry of the periodic atomic configuration, they should behave as extended elastic scatterers for the 2D Bloch electrons. Indeed, it has been demonstrated that steps in the SIC region act as a Josephson barrier in the

superconducting phase [10, 30]. The disruption of the proximity effect is thus due to the poor transmission of electrons through the barrier at the step edges.

In the upper-left part of the STM image of Fig. 2(a), there is a Pb island directly contacted to the SIC phase underneath. Since a downward step edge is close to the island, the terrace width of the sandwiched SIC area is quite narrow, less than the coherence length of the normal metal. We found that in such confined area the proximity effect is enhanced, as shown in the enlarged ZBC map in Fig. 3(a). Figure 3(b) displays several cross-sectional ZBC profiles taken in the areas with various terrace widths. The plots clearly show that the DOS at E_F in the confined area is more suppressed compared to the flat terrace (See Table 1 for the values). For the narrowest terrace (12.8 nm) in Fig. 3(b), for instance, the amount of the ZBC at the SN interface is ~ 1/3 of the flat SIC area.

The enhancement of the gap or the correlated pair density by the presence of the step is explained by a mechanism called reflectionless tunneling [31, 32], which is caused by elastic scattering due to the barrier at the step edge. Elastic scattering redirects Andreev-reflected electrons/holes toward the SN interface, making a loop in their trajectories with the SN interface. Because of the constructive quantum interference due to the phase-conjugated nature of the Andreev reflection, the formation of the loop enhances the probability of multiple Andreev reflection and the proximity effect as well [31, 32]. As the Andreev-reflected quasiparticles can tunnel through the interface without reflection, the enhancement is called reflectionless tunneling.

The presence of the potential barrier and electron scattering at the step edge imply electrical resistance. In order to obtain information on the conductivity of the surface step we calculated the ZBC profiles using the Usadel equation and compared them with experiments. It has been reported that reflectionless tunneling can be discussed using the Usadel equation [33]. For the calculation we considered a model composed of three regions: superconductor / normal metal / normal metal (SNN), as depicted in Fig. 3(c), similar to the double-barrier junction model [34]. The width of the sandwiched normal metal corresponds to the terrace width. In the SNN model, in addition to the conductivity ratio at the SN interface σ_{SN}/σ_N, we introduced the conductivity ratio at the NN boundary σ_{NN}/σ_N as parameter. Here σ_{NN} is the

conductivity through the abutting normal metals, that is, step conductivity in the normal metal. All the other parameters were set at the same values as those of Fig. 1(c). As shown in Fig. 3(b), the calculated ZBC profiles show good agreement with experiments.

The conductivity ratios at the NN step (σ_{NN}/σ_N) and the SN interface (σ_{SN}/σ_N), obtained from comparison between model calculations and experiments, are listed in Table 1. The step conductivity ratio σ_{NN}/σ_N was estimated as $10.9\pm3.9\ \mu m^{-1}$ from the terraces whose width is less than ξ; for the wider terraces (54.3 nm and 76.7 nm) the weak pair correlation at the step results in large uncertainties in σ_{NN}/σ_N. From the ratio we noticed that the contribution of the step resistance to the total surface resistance is significant. In the case of the stepped area shown in Fig. 2(a) (~11 steps/μm corresponding to the tilting of 0.20°), which was observed on a nominally (111)-oriented substrate, the step resistance contributed almost 50% of the total resistance in the direction perpendicular to the step edges. If we assume that the reported 2D sheet conductivity of the SIC phase (0.77 mS/□) [2] does not include the contribution of steps, the step conductivity is given as $(0.84\pm0.30)\times10^4$ S/m.

The conductivity through single ML-high steps has been measured in various techniques. Four-probe transport measurements [35-37] on vicinal surfaces in principle can provide an estimate of the step conductivity by dividing measured conductances with step density, but it has been possible only for samples with low step resistivity like Ge(111)β(√3×√3)-Pb surface [36]. Eliminating conductances through the bulk and subsurface layers is another challenge [37], as discussed in the step resistivity measurements of Si(111)7×7 surface. Using microscopic techniques, the step resistivity was estimated through the observation of standing waves by STM [35], but the method is applicable only to ballistic systems. Scanning tunneling potentiometry [38, 39] has been the only microscopic method applicable to diffusive systems. Since the method detects potential profiles under macroscopic current flow, an ambiguous estimate of the current density may cause uncertainty in the conductance measurements. Here, we measured in a truly microscopic and local fashion the effect of a single step on the conductivity in diffusive normal metal. Our method is new for characterizing transport properties of single nano-scale structures, which is not accessible by other methods.

Compared with the step conductivity ratio, σ_{SN}/σ_N exhibits systematic variation

with the terrace width. This implies other physical causes besides reflectionless tunneling. One possible candidate for the variation is the pair potential Δ induced by the proximity effect. [11, 40] Due to the proximity effect the pair correlation is induced in the normal metal, but the pair potential Δ, which is a product of the pairing interaction, DOS, and the correlated pair density, is small in a metal because the pairing interaction is weak. The agreement, shown in Fig. 1(c), between the experimental and calculated spectra (Usadel equation without Δ in the normal metal) indicates that the effect of Δ is small or effectively incorporated into the SN interfacial parameter, as was the case of previous work on the same system. [8] In a situation just above the critical temperature of the normal metal, where the pairing interaction is strong and the pair density is large (*eg*. by reflectionless tunneling), the induced Δ may not be negligible and therefore enhance the superconducting pair correlation [11, 40]. Since Δ in the normal metal is assumed zero in our calculation, the σ_{SN}/σ_N values are overestimated for narrow terraces, and the amount of the overestimation becomes larger for narrower terraces, which is consistent with the results shown in Table 1. (See Sec. 5 in the SM for details [23]). From the results of wide terraces, where the enhancement due to Δ is less than that for narrow terraces, the effective SN interfacial conductivity ratio σ_{SN}/σ_N is estimated as $39\pm6.5\ \mu m^{-1}$, comparable with that for Fig. 1. On the other hand, σ_{NN}/σ_N is basically determined by the boundary condition at the step edges (eq. S4 in SM), where the correlated pair density and therefore Δ are not presumably large. Since the obtained σ_{NN}/σ_N is not sensitive to the variation of σ_{SN}/σ_N as shown in Table 1, the ZBC profiles near the step edges should provide a good measure of the step conductivity.

We also found in the ZBC map (Fig. 2(b)) that the DOS in the SIC layer just outside the edge of Pb islands is not uniform, which is in contrast with cases of flat metallic layers [8,11,13,14]. The site marked A, where the edge of the Pb island is directly situated on a terrace of the SIC phase, exhibits strong proximate effect, whereas at site B (C), where the edge of the island coincides with the upward (downward) step of the substrate, the proximate effect is intermediate and weak among the three sites (See Sec. 4 in SM for details [23]). The difference in ZBCs across the SN interface is a measure of the electronic transparency across the interface, closely related to σ_{SN}. [41] Site A has large transmission probability because of the direct contact. At site B, an

atomically thin contact is formed between a Pb island and the SIC phase. At site C, on the other hand, a Pb island is separated from the SIC phase by an atomic step. The ZBC mapping thus demonstrates the spatial distribution of the SN conductivity and tells us that the intensity of the proximity effect depends on the atomistic contact configuration at the SN interface. [41].

In conclusion, using low-temperature STM/STS, we have investigated transport properties through a surface step of the SIC phase by utilizing the superconducting pair correlation. We found that surface steps in the 2D metallic layer have significant influence on the propagation of the induced pair correlation. They disrupt its propagation and enhance superconductivity near the interface via reflectionless tunneling. However, we found no minigap. The observed results are explained by elastic scattering at the steps in the framework of the Usadel equation. Through the SNN model calculations we obtained the electronic conductivity through a single ML-high surface step and found that the step resistance is dominant in the total surface resistance even for nominally flat surfaces. Our scanning probe method is truly microscopic. It is suitable for characterizing local transport properties of nanostructured disorder in diffusive 2D metallic layers. We also expect that improved understanding of the role of steps on the proximity effect can open new paths for engineering atomic-scale superconducting quantum devices.

Acknowledgements

We appreciate fruitful discussions with Yasuo Yoshida, Masaru Okada, Kazuo Ueda, Nobuhiko Hayashi, Mahn-Soo Choi, Dimitri Roditchev, Michael Tringides, and Ing-Shouh Hwang. This work was supported by JSPS KAKENHI Grant (Nos. 21360018 and 25286055). Work at Los Alamos National Laboratory was supported through the U.S. DOE contract No. DE-AC52-06NA25396 by the LDRD program (SZL) and in the early stage by the Office of Basic Energy Sciences, Division of Materials Sciences and Engineering (MJG).

Reference

[1] T. Zhang, *et al.*, *Nature Phys.* **6**, 104 (2010).

[2] M. Yamada, T. Hirahara, and S. Hasegawa, *Phys. Rev. Lett.* **110**, 237001 (2013).

[3] T. Uchihashi, P. Mishra, M. Aono, and T. Nakayama, *Phys. Rev. Lett.* **107**, 207001 (2011).

[4] K. Yaji, *et al.*, *Nat. Commun.* **1**, 17 (2009).

[5] D.V. Gruznev, *et al.*, *Scientific Reports* **4**, 4742 (2014).

[6] A. V. Matetskiy, et al., *Phys. Rev. Lett.* **115**, 147003 (2015).

[7] K. Sakamoto, *et al. Nature Comm.* 4, 2073 (2013).

[8] J. Kim, *et al.*, *Nature Phys.* **8**, 464 (2012).

[9] L. Serrier-Garcia, *et al.*, *Phys. Rev. Lett*. **110**, 157003 (2013).

[10] C. Brun, *et al.*, *Nature Phys.* **10**, 444 (2014).

[11] V. Cherkez, *et al.*, *Phys. Rev. X* **4**, 011033 (2014).

[12] D. Roditchev, *et al.*, *Nature Physics* **11**, 332 (2015).

[13] A. Stępniak, *et al*. *AIP Advances* **5**, 017125 (2015).

[14] F. D. Natterer, *et al.*, *Phys. Rev. B* **93**, 045406 (2016).

[15] D. Eom, S. Qin, M. Y. Chou, and C. K. Shih, *Phys. Rev. Lett.* **96**, 027005 (2006).

[16] T. Nishio, *et al.*, *Phys. Rev. Lett.* **101**, 167001 (2008).

[17] G. Koren, *et al.*, *Europhys. Lett.* **103**, 67010 (2013).

[18] A. C. Keser, V. Stanev, and V. Galitski, *Phys. Rev. B* **91**, 094518 (2015).

[19] L. Fu and C. L. Kane, *Phys. Rev. Lett.* **100**, 096407 (2008).

[20] V. Mourik, *et al.*, *Science* **336**, 1003 (2012).

[21] S. Nadj-Perge, *et al.*, *Science*, **346**, 602 (2014).

[22] J.-P. Xu, *et al. Phys. Rev. Lett.* **114**, 017001 (2015).

[23] See Supplemental Material at http://link.aps.org/supplemental/XXX for a description on surface properties and superconductivity, diffusion constant and mean free path, the Usadel equation, site dependence of ZBC, and reflectionless tunneling and the induced pair potential, which include Refs. 42 and 43.

[24] K. Horikoshi, X. Tong, T. Nagao and S. Hasegawa, *Phys. Rev. B* **60** 13287 (1999).

[25] B. Sacépé, *et al.*, *Nat. Commun.* **1**, 140 (2010).

[26] C. Brun, *et al.*, *Phys. Rev. Lett.* **108**, 126802 (2012).

[27] K. D. Usadel, *Phys. Rev. Lett.* **25**, 507 (1970).

[28] W. Belzig, C. Bruder, and G. Schön, *Phys. Rev. B* **54**, 9443 (1996).

[29] Ya. V. Fominov and M. V. Feigel'man, *Phys. Rev. B* **63**, 094518 (2001).

[30] S. Yoshizawa, *et al.*, *Phys. Rev. Lett.* **113**, 247004 (2014).

[31] B. J. van Wees, P. de Vries, P. Magnée, and T. M. Klapwijk, *Phys. Rev. Lett.* **69**, 510 (1992).

[32] T. M. Klapwijk, *J. Supercond. Novel Mag.*, **17**, 593 (2004).

[33] Y. Tanaka, A. A. Golubov, and S. Kashiwaya, *Phys. Rev. B* **68**, 054513 (2003).

[34] A. F. Volkov, A. V. Zaitsev, and T. M. Klapwijk, *Physica C* **210**, 21 (1993).

[35] I. Matsuda, *et al.*, *Phys. Rev. Lett.* **93**, 236801 (2004)

[36] S. Hatta, T. Noma, H. Okuyama, and T. Aruga, *Phys. Rev. B* **90**, 245407 (2014).

[37] S. Just, *et al.*, *Phys. Rev. Lett.* **115**, 066801 (2015).

[38] J. Homoth, *et al.*, *Nano Lett.* **9**, 1588 (2009).

[39] B.V. C. Martins, M. Smeu, L. Livadaru, H. Guo, and R. A. Wolkow, *Phys. Rev. Lett.* **112**, 246802 (2014).

[40] M. Wolz, C. Debuschewitz, W. Belzig, and E. Scheer, *Phys. Rev. B* **84**, 104516 (2011).

[41] G. E. Blonder, M. Tinkham, and T. M. Klapwijk, *Phys. Rev. B* **25**, 4515 (1982).

[42] W. H. Choi, H. Koh, E. Rotenberg, and H. W. Yeom, *Phys. Rev. B* **75**, 075329 (2007).

[43] L. Seehofer, G. Falkenberg, D. Daboul, and R. L. Johnson, *Phys. Rev. B* **51**, 13503 (1995).

Figure and table captions

Figure 1: (a) 3D-rendered STM image showing an interface between an 8-ML Pb island and a SIC phase formed on a Si(111) substrate. The probed area is 200 × 200 nm^2. For imaging the tunneling current I_T and sample bias voltage V_S were set at 30 pA and +50 mV, respectively. A characteristic striped pattern can be seen in the SIC phase. (inset) Color-coded 200 tunneling spectra taken along the 200 nm-long line from the Pb island to the SIC phase drawn in (a). (b) Negative ZBC profile normalized by the value measured at 200 nm away from the SN interface. The red line is a fitted exponential function with decay length of 40.5 nm. (c) Tunneling conductance (*dI/dV*) spectra taken on the Pb island and in the SIC area at 1, 20, 47, 80, 110, 139, 178 nm from the SN interface (colors), and calculated DOS spectra solving the Usadel equation (white lines). Each line is offset vertically by 0.8 for clarity.

Figure 2: (a) STM image of Pb islands formed on a SIC-phase-covered Si(111) substrate (1.0 μm square, I_T = 50 pA and V_S = 50 mV). The edges of the Pb islands and the steps of the SIC phase are highlighted with white and black dashed lines, respectively. (b) ZBC color map of the same area as (a). (c) Normalized negative ZBC (upper) and topographic (bottom) profiles taken along the line aa' drawn in (b). The vertical dashed lines in red, green, and blue correspond to the positions of a normal metal step, the SN interface, and a step of the substrate embedded under the Pb island, respectively.

Figure 3: (a) 400 nm × 400 nm ZBC colored map taken in area that includes a narrow terrace sandwiched by an edge of a Pb island and a step edge of the SIC phase. The edges of Pb islands and the SIC steps are highlighted with white and black dashed lines, respectively. (b) Normalized negative ZBC profiles across the SN interface and the step edges measured along the colored lines drawn in (a). The length written on each plot is the terrace width measured along the corresponding line. The whitish-colored lines are theoretical curves based on the Usadel equation calculated in the SNN model. (c) Schematics of the SNN model.

Table 1: normalized ZBC values measured at the SN interface, and ratio of conductivities at the normal metal NN step, σ_{NN}/σ_N, and at the SN interface, σ_{SN}/σ_N,

obtained from the fitting shown in Fig. 3(b).

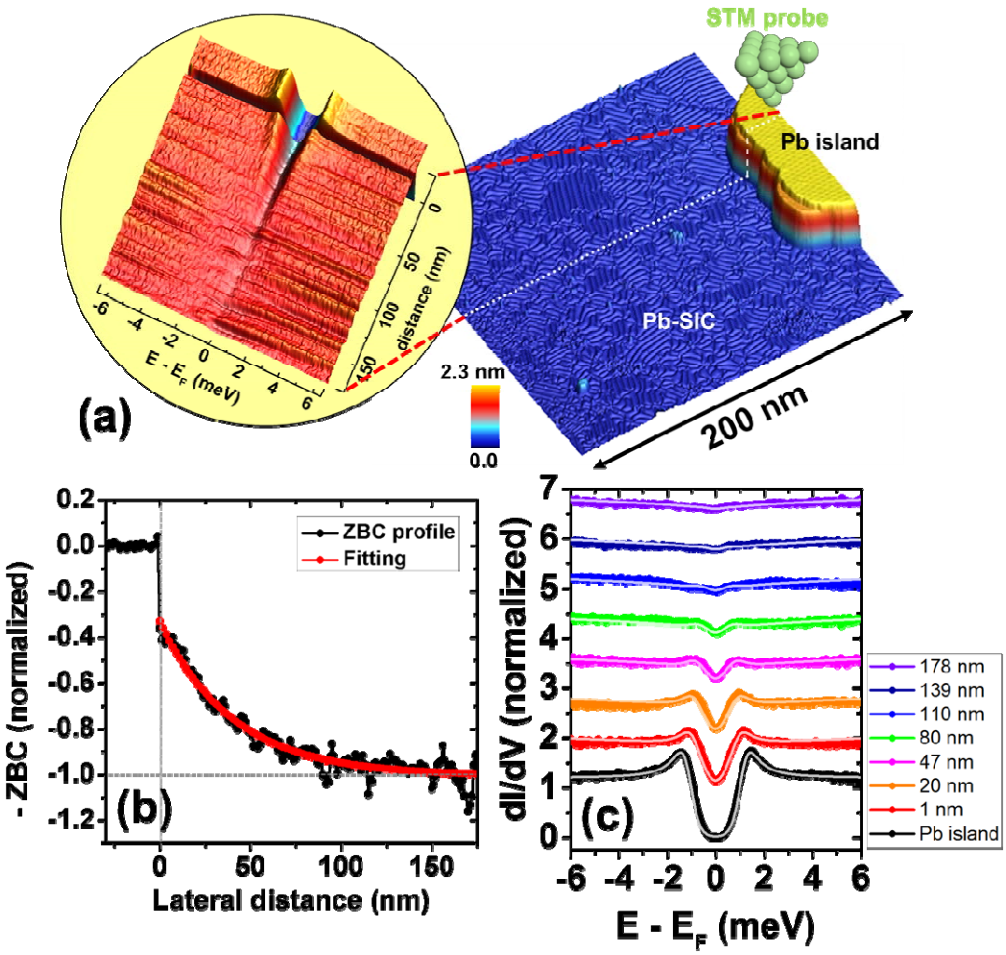
STM probe
Pb island
Pb-SiC
200 nm
2.3 nm
0.0
(a)
E - E_F (meV)
distance (nm)
(b)
- ZBC (normalized)
ZBC profile
Fitting
Lateral distance (nm)
(c)
dI/dV (normalized)
E - E_F (meV)
178 nm
139 nm
110 nm
80 nm
47 nm
20 nm
1 nm
Pb island

Figure 1

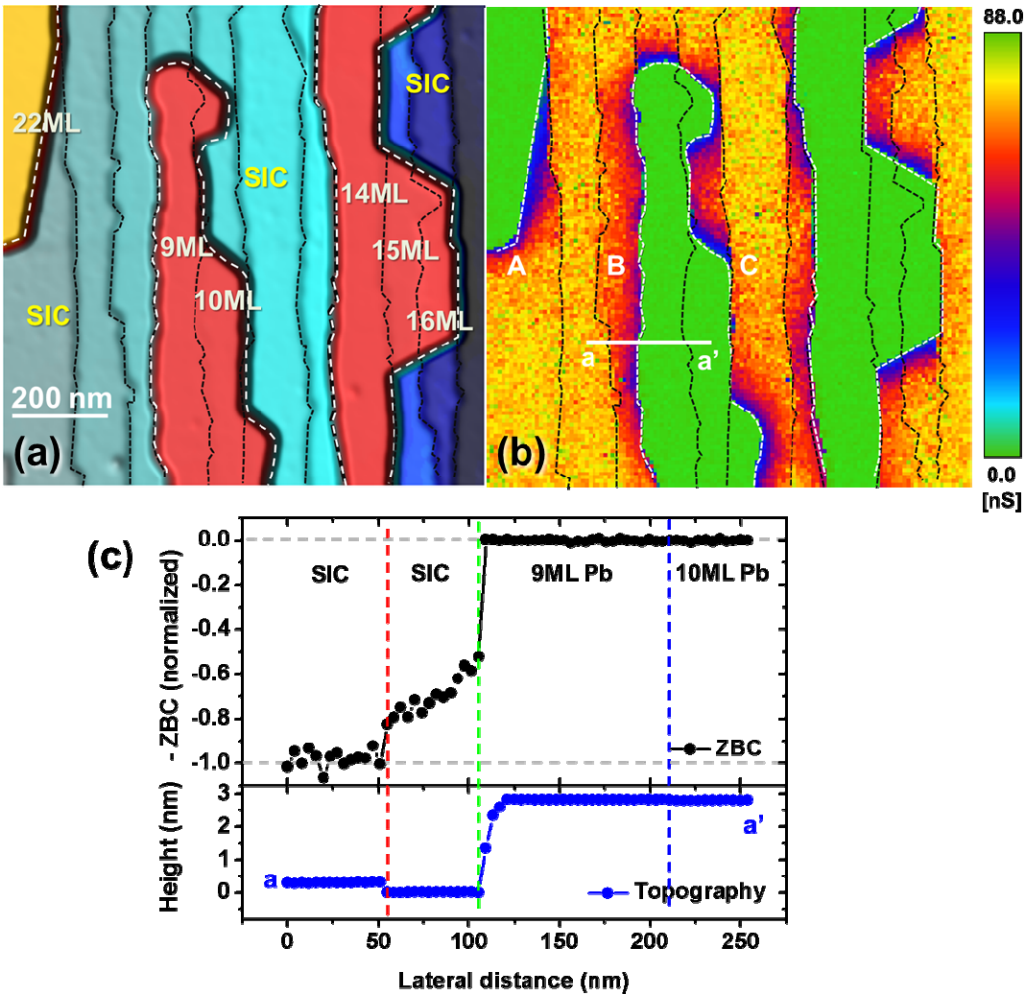
22ML
SIC
SIC
14ML
9ML
15ML
10ML
SIC
16ML
200 nm
(a)
A
B
C
a
a'
(b)
88.0
0.0
[nS]
(c)
SIC
SIC
9ML Pb
10ML Pb
ZBC
- ZBC (normalized)
Height (nm)
a
a'
Topography
Lateral distance (nm)

Figure 2

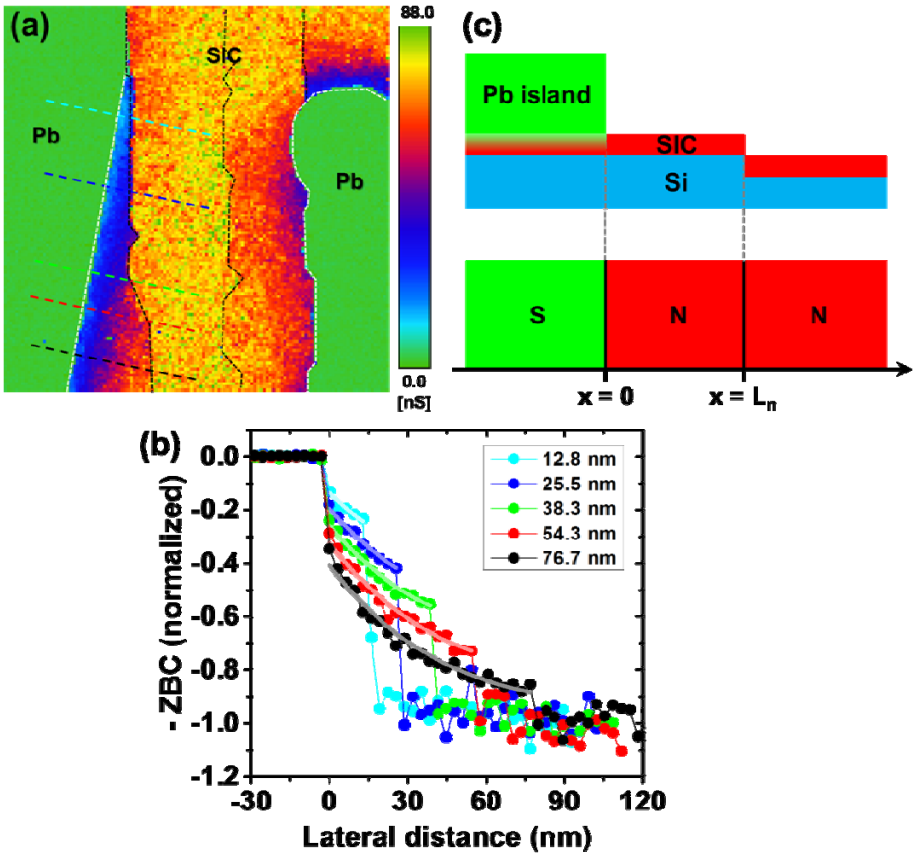
(a)
SiC
Pb
Pb
88.0
0.0
[nS]
(c)
Pb island
SIC
Si
S
N
N
x = 0
x = L_n
(b)
- ZBC (normalized)
0.0
-0.2
-0.4
-0.6
-0.8
-1.0
-1.2
-30
0
30
60
90
120
Lateral distance (nm)
12.8 nm
25.5 nm
38.3 nm
54.3 nm
76.7 nm

Figure 3

terrace width (nm)	12.8	25.5	38.3	54.3	76.7
normalized ZBC at the SN interface	0.13	0.18	0.24	0.29	0.35
σ_{NN}/σ_N (μm^{-1})	10.4±3.9	11.8±2.5	10.4±4.7	13^{+8}_{-4}	26^{+87}_{-14}
σ_{SN}/σ_N (μm^{-1})	70±18	58±6.5	47±9	42±6.5	35±5

Table 1